Approaches to the remote mapping of vehicle noise sources in a reverberant environment

A. Papaioannou[1], S. Elliott[1], J. Cheer[1]
[1] Institute of Sound and Vibration Research
University Road, SO17 1BJ, Southampton, UK
e-mail: **A.Papaioannou@soton.ac.uk**

Abstract
In this paper, new methods for the remote acoustic source mapping of vehicle noise sources are considered. This work initially considers the effect of a wall reflection on conventional methods of processing the signals from a remote microphone array. The use of alternative array processing techniques to discriminate against the reflections are then considered and used, to produce a 'heatmap' of the array response as a noise source is moved around within the chamber. In a first step, an inverse impedance weighting strategy is considered, to distinguish the desired physical source location from the one created due to the reflections. In a second step, additional restrictions are also taken into account such as the ability of the microphone array to suppress the high levels for sources close to the microphones and an optimised weighting strategy is introduced and applied.

1 Introduction

The exterior sound emission of a vehicle is an increasingly important criterion for the homologation of road vehicles. The latest limit value of 74 dB(A) is already a major challenge for car manufacturers and an even lower limit of 68 dB(A) is in plan for the near future. Therefore, measurement of the drive-by noise of vehicles is important to ensure lower sound levels for people living close to roads. Until recently, it has been measured outdoors according to ISO – 362-1:2015, [1]. However, drive-by noise can now be estimated in a laboratory environment, with a stationary vehicle on a rolling road, [2], by processing and identifying the individual sources of noise on the vehicle and then synthesising the pressures that would be measured in a drive-by test, [3-4]. Within this method, the tire-road noise is separately energetically added to the powertrain noise and the final result is compared to the outdoor measurement, [5-6].

The indoor estimation of pass-by noise has advantages over outdoor measurements in terms of the repeatability and robustness of the measurements. However, the use of chambers with imperfectly anechoic walls can distort the results in certain frequency bands. With the aim of overcoming this limitation, new approaches to the mapping of the vehicle pass-by noise sources in a reverberant environment are developed in this paper, utilising optimal beamforming.

2 Formulation

As a first step, we may assume that a specific noise source on the vehicle can be represented by a compact monopole source radiating omnidirectionally. If a microphone is positioned a distance of r from the source, the pressure is, [7],

$$p_i(r) = Z_i(r)q = j\omega\rho_0 q\frac{e^{-jkr}}{4\pi r} \quad \text{(Pa)} \tag{1}$$

Where Z_i is the transfer impedance and q is the source strength.

Assuming an array of 41 microphones positioned on a line 7.5 m away from the source and a rigid wall 3 meters behind it, then the contributions due to the various reflections from the wall could be modelled as an image source, placed 13.5 meters away from the linear array, as shown in Figure 1.

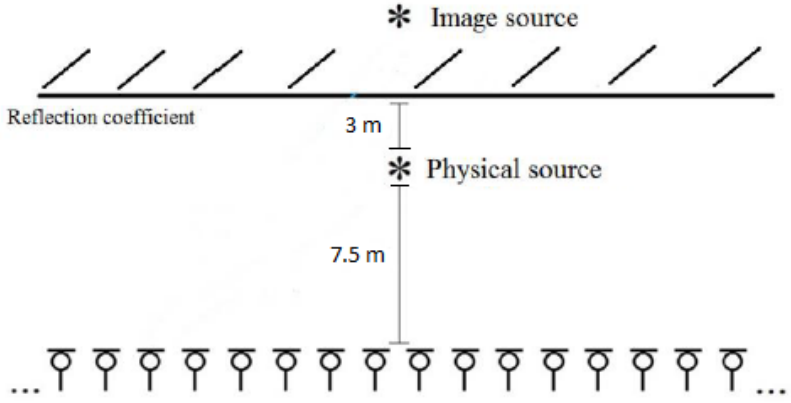

Figure 1: Environment of pass-by noise measurement with a rigid wall

The array output due to the source at each point is initially calculated by adding the contributions from each microphone together, so that

$$\mathrm{p(x)} = \frac{1}{41}\sum_{\mathrm{i=1}}^{41} \mathrm{p_i(x)} \quad \text{(Pa)} \tag{2}$$

This uniform weighting corresponds to that of a broadside array using a delay and sum beamformer with a far-field directivity pointing towards the source. The pressure can also be expressed in terms of the Sound Pressure Level (SPL), which is given as

$$\mathrm{SPL(x)} = 20\log_{10}\left(\frac{\mathrm{p_{rms}(x)}}{\mathrm{p_{ref}}}\right) \quad \text{(dB)} \tag{3}$$

So that SPL is independent of the phase of *p(x)* and hence the frequency. In this case, p_{ref} is chosen to be the array output pressure when the source is positioned at the physical source location in Figure 1. By moving the source around the room, a heatmap in terms of the sound pressure level at each point can be created, as shown in Figure 2. From this plot, it can be seen that the uniform linear array generates a high estimate of the SPL in the near field of the array.

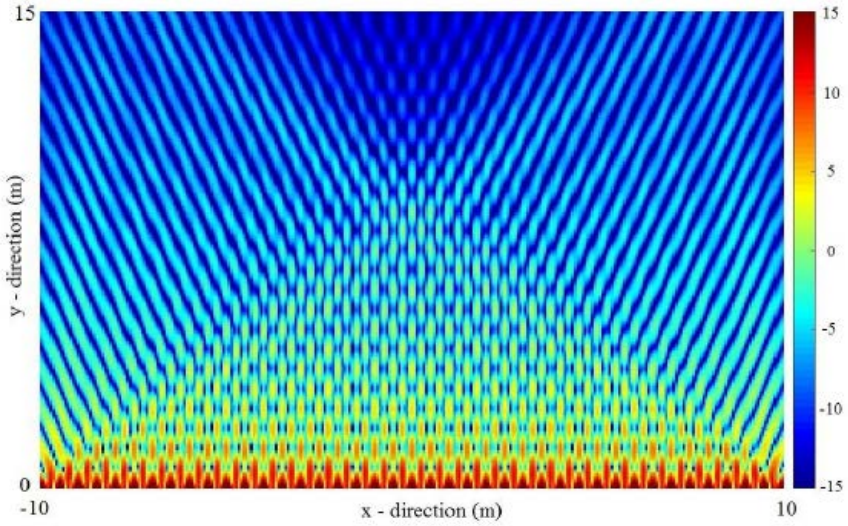

Figure 2: Heatmap of the sound pressure level due to a monopole source measured using a 41 – microphone array (1 kHz) and the uniform weighting method

To provide further insight into those results, Figure 3 shows the Sound Pressure Level estimated along the x = 0 axis, moving away from the array towards the physical source location at x = 7.5 m and the image source at 13.5 m for various working frequencies.

It can be seen that the response of the array to the image source is approximately 10 dB less than the one to the physical source, and hence the image source will significantly alter the estimate of the source strength. It is also shown in Figure 3 that the weighting strategy offers poor results at very low frequencies below around 100 Hz and only delivers 4 and 8 dB level difference between the physical and image source points at 50 and 100 Hz respectively. To overcome these limitations, the next step is to apply appropriate weighting to the microphones in order to achieve further discrimination against the image source strength and points close to the array.

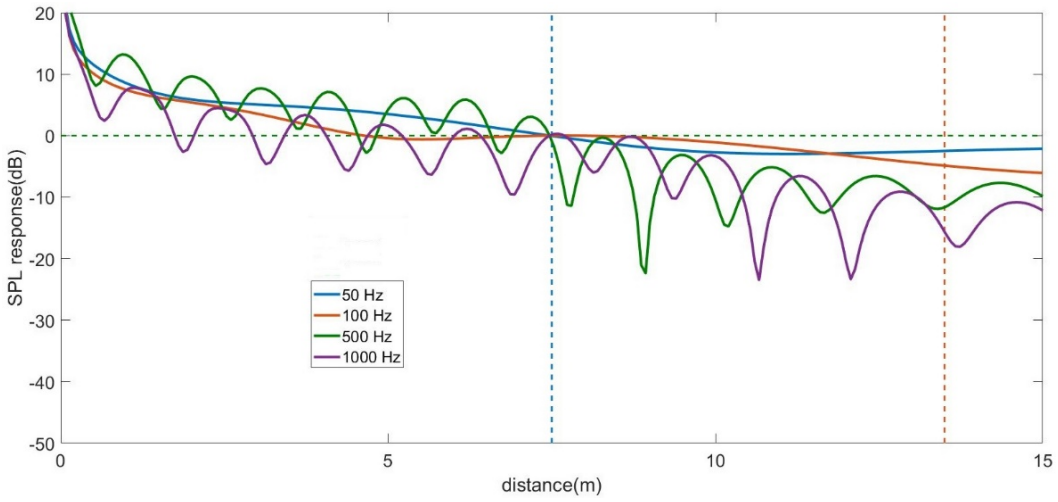

Figure 3. Sound pressure level at x = 0 m over distance in the y – direction using the uniform weighting for f = 50, 100, 500, 1000 Hz

3 Inverse impedance weighting synthesis

A simple method of weighting the microphones would be to use the inverse of the impedance measured when the source is placed at y = 7.5 m, x = 0 m. The heatmap is then constrained to deliver unity gain for the point where the physical source is placed. The weights are, thus, equal to

$$w_i = \frac{1}{Z_{i,y=7.5,x=0}} \tag{4}$$

Where $Z_{i,y=7.5,x=0}$ is the impedance between the i-th microphone and the physical source position. The overall output of the array is then equal to the sum of the weighted pressures

$$p(x) = \frac{1}{41}\sum_{i=1}^{41} w_i p_i(x) \quad \text{(Pa)} \tag{5}$$

Since all terms, $w_i p_i(x)$, in this symmetry are equal to unity when the source is at the reference position, x = 0, y = 7.5 m, this array processing strategy is similar to the one used in the far-field delay-and-sum approach. As a result, the heatmap in terms of the sound pressure level is transformed, as shown in Figure 5. From this plot, it can be seen that the physical source SPL is at 0 dB, as enforced, and the level elsewhere is significantly attenuated compared to the uniformally weighted array results in Figure 4. For reference, the amplitude and the phase of the array weights used to produce the heatmap in Figure 5 are shown in Figure 6(a), (b). From the plots, it can be seen that the inverse impedance weighting scheme results in array shading that compensates for the path length differences between the physical source and each of the array microphones.

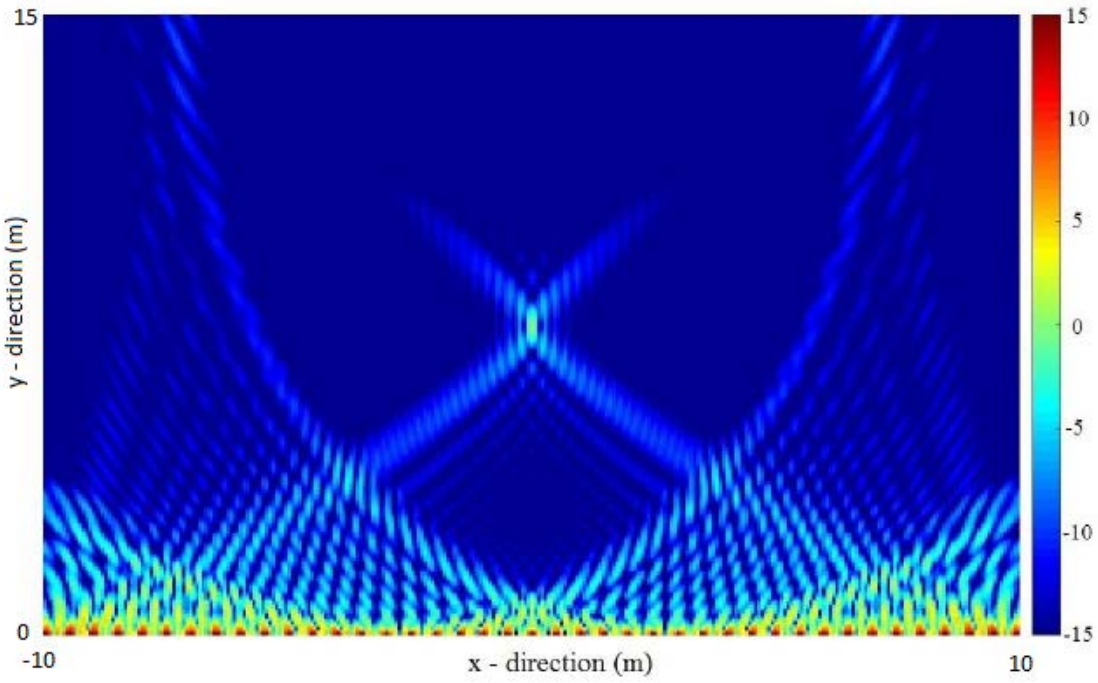

Figure 4. Heatmap in terms of the sound pressure level for a monopole source with a 41 – microphone array (1 kHz) using the inverse impedance weighting

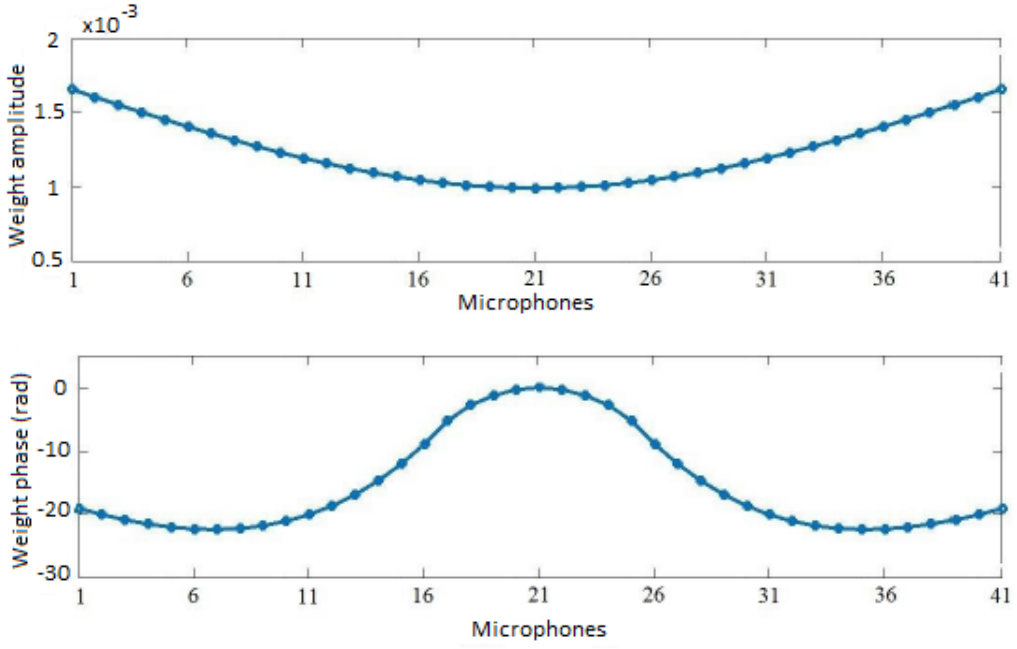

Figure 5(a), (b). Amplitude and phase of the inverse impedance weights

To provide a clear picture of the results presented in Figure 5, the sound pressure level is again plotted along y-axis at x = 0 m at four discrete frequencies. From these results, it can be seen that, at 1 kHz, the weighting provides a 23.5 dB level difference between the physical and the image source (assuming that there is no noise absorption provided by the rigid wall), while retaining the physical source level at unity gain. However, the level is very high (up to 30 dB) when the source is placed very close to the array. The method is also limited at low frequencies around 100 Hz and only delivers a level of difference of 3 and 9 dB between the physical and image source points at 50 and 100 Hz, as shown in Figure 6.

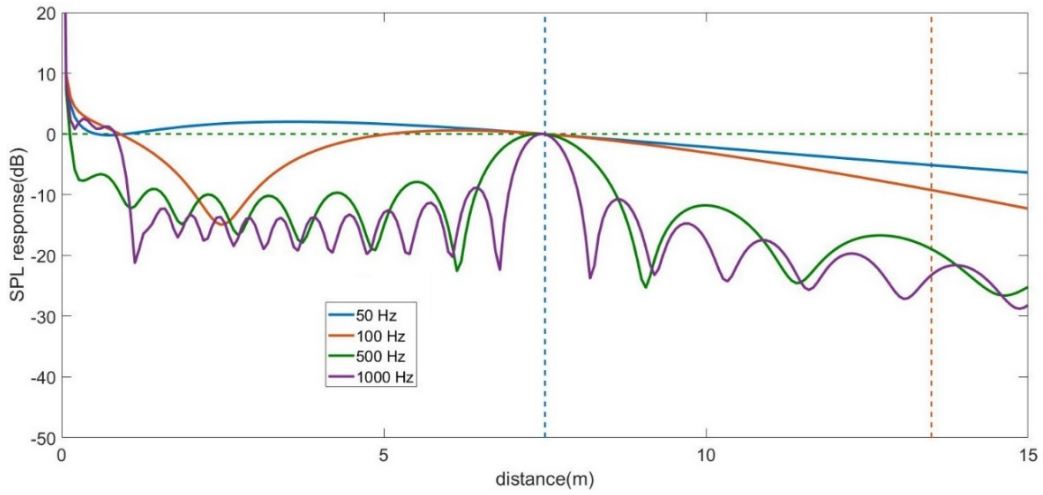

Figure 6. Sound pressure level at x = 0 m over distance in the y – direction using the inverse impedance weighting for f = 50, 100, 500, 1000 Hz

4 Optimised weighting synthesis

In an attempt to overcome the limitations highlighted on the inverse impedance weights, an alternative strategy that directly optimises the array weights will be presented in this section. In this case, the microphone array weights are specified by performing a linear optimisation of the weights w_i subject to three constraints:

- The weights provide unity gain for the physical source position i.e. $p_{y=7.5,x=0} = \frac{1}{41}\sum_{i=1}^{41} w_i p_i = 1$
- The weights provide zero gain for the image source position i.e. $p_{y=13.5,x=0} = \frac{1}{41}\sum_{i=1}^{41} w_i p_i = 0$
- The weights are kept to the minimum magnitude possible in order to discriminate against the positions close to the microphone array i.e. $min \sum_{i=1}^{41} |w_i|$

The weight calculation is split into two parallel optimisation problems in Matlab. The first one solves the least-squares curve fitting problem of the form $min \frac{1}{2}\left[\frac{1}{41}\sum_{i=1}^{41} w_i p_i - 1\right]_2^2$ subject to $\frac{1}{41}\sum_{i=1}^{41} w_i p_i = 0$. The second one adds the supplementary constraint $min \sum_{i=1}^{41} |w_i|$ by setting numerical bounds on each w_i. The function used utilises the method of the Lagrange multipliers which is a strategy for finding the local maxima and minima of a function subject to equality constraints [44]. The only prerequisite is that the used functions have continuous first partial derivatives as is the case in the considered problem..

To assess the performance of this weights optimisation process, the total pressure at each source point is again estimated using Equation 5, but with the calculated w_i. The heatmap in terms of the sound pressure level is shown in Figure 7 and the corresponding amplitude and phase of the optimised array weights are shown in Figure 10(a) and 10(b) respectively. It is interesting to see from both the amplitudes of the array weights and the heatmap in Figure 7 that this optimisation method effectively creates two separate arrays at either end of the microphone array, both focused on the physical source location. It can be seen from Figure 7 that this results in an effective triangular – type array behaviour.

To provide a consistent analysis of this array processing method, the sound pressure level is plotted along the y-axis at x = 0 m in Figure 9 with lines indicating the positions where the physical and image sources are located. At 1 kHz, it can be seen from Figure 9 that the weighting creates a 43.1 dB level difference between the physical and the image source (assuming there is no sound absorption by the rigid wall), while retaining the physical source level slightly lower than unity gain (-0.6 dB). As a result, the optimized weighting enhances the level difference between the two source points by about 20 dB compared to the inverse impedance weighting strategy. However, the optimized weighting also discriminates against the source points close to the microphone array reducing the level from 30 dB to -18 dB. In principal, there would be no signal for a source at the image location if the optimization problem

above was satisfied, but the finite level difference illustrates that the optimisation problem does not have a solution, particularly at low frequencies, as shown in Figure 9. In particular, it can be seen that the weighting strategy offers poor results in very low frequencies only delivering 4 to 8 dB level difference between the physical and image source points at 50 and 100 Hz.

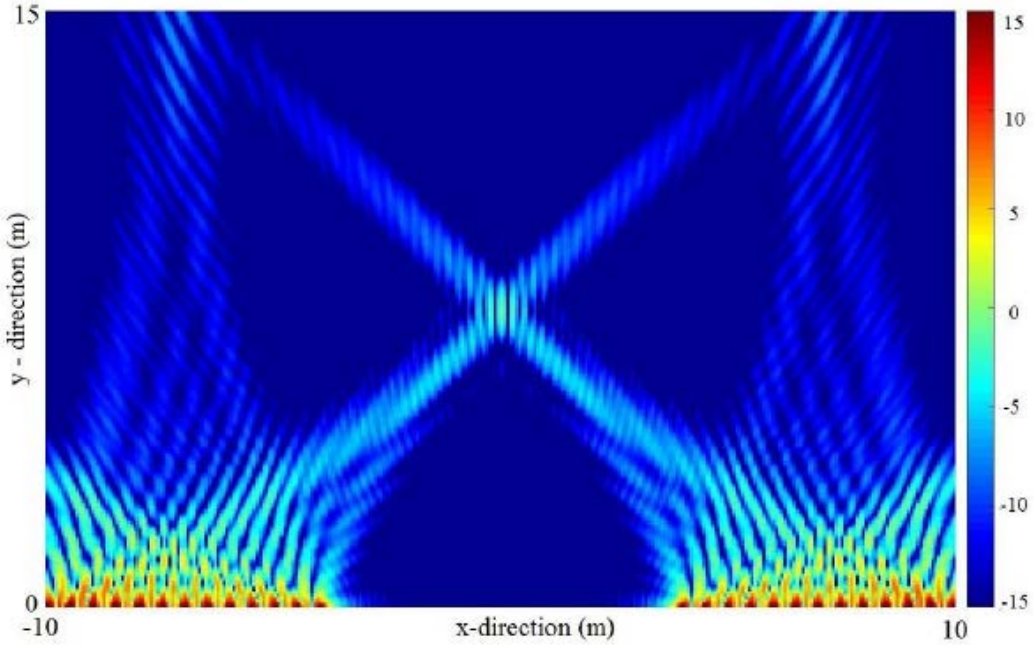

Figure 7. Heatmap in terms of the sound pressure level for a monopole source with a 41 – microphone array (1 kHz) using the optimised weighting

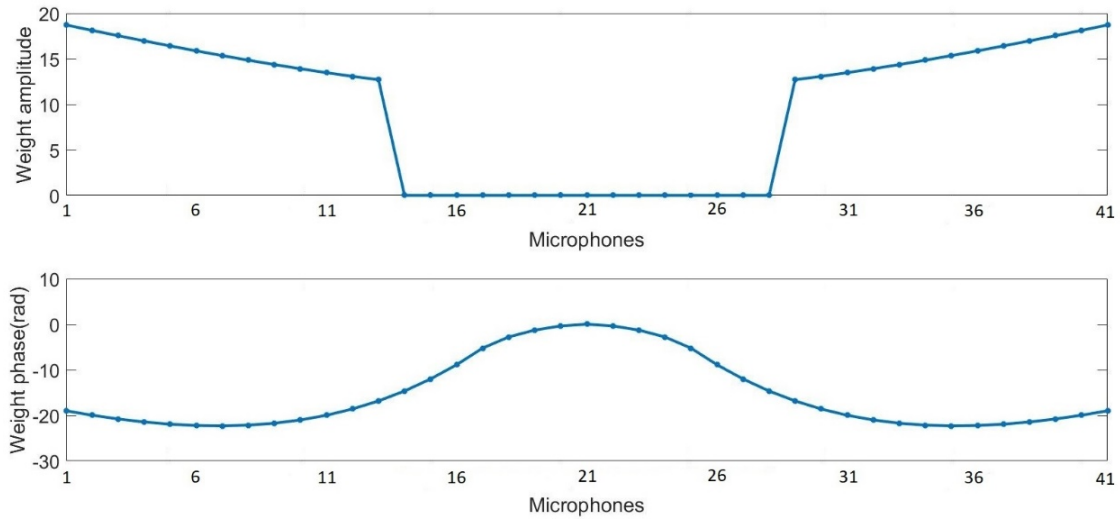

Figure 8(a), (b). Amplitude and phase of the optimised weights

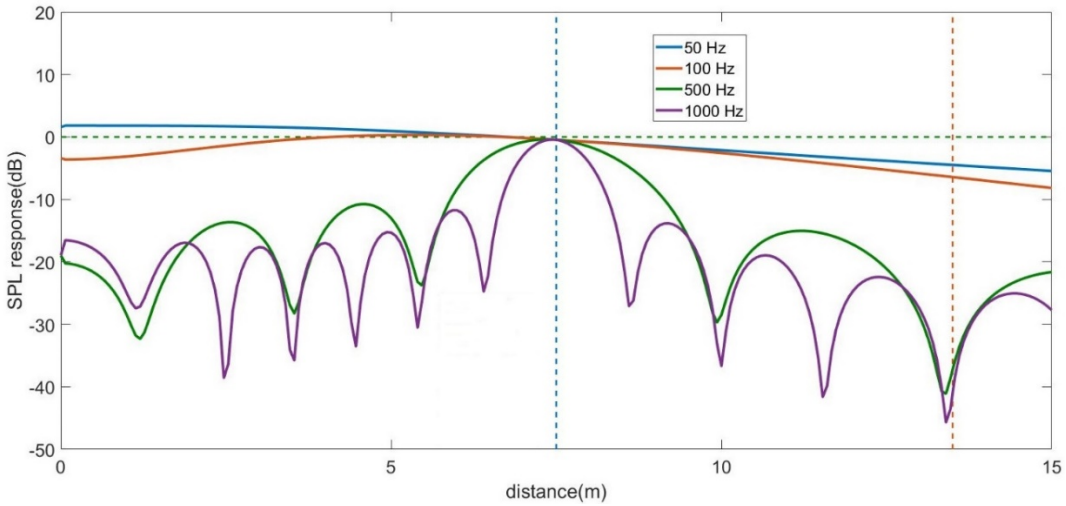

Figure 9. Sound pressure level at x = 0 m over distance in the y – direction using the optimised weighting for f = 50, 100, 500, 1000 Hz

To provide a clear comparison between the three considered array weighting methods, Figure 13 shows the difference between the physical and image source strengths for the three different weighting strategies, which correspond to the discrimination that the array provides against the image source. It should be noted that in contrast to the uniform array weighting, the inverse impedance and optimised weighting assume a known position for the image source, and so the results will be degraded if the position of the physical source with respect to the wall is not exactly where it is assumed to be in Figure 1. Nevertheless, at frequencies above 100 Hz, the inverse impedance method achieves a significant performance increase, with a 10 dB discrimination between 2 and 10 kHz, whilst the optimised weighting achieves a performance increase of about 25 dB over the same frequency range.

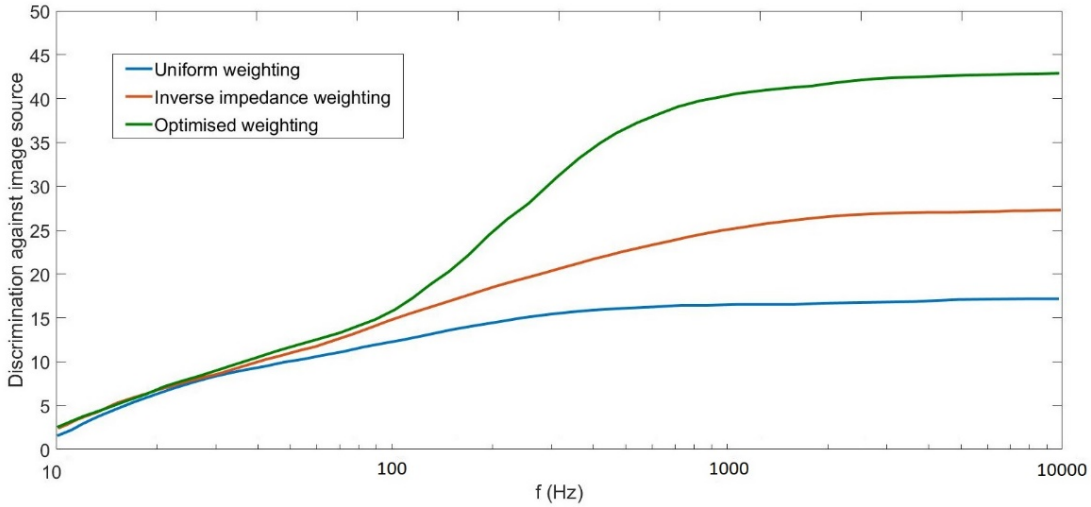

Figure 10: Difference between the level at the assumed image source and that at the physical source for the 3 different array weighting methods

5 Conclusions

In this paper, new approaches to the acoustic source identification for the synthesis of vehicle pass-by noise sources have been considered. The effect of a wall reflection on conventional methods of processing the signals from the far field microphone array has been examined and two alternative array processing

techniques to discriminate against the reflections are considered. A ‘heatmap’ of the array response as a noise source is moved around within the measurement chamber has then been produced, while two different weighting strategies are considered to distinguish the desired physical source location from the one created due to the reflections. Additional restrictions are also taken into account such as the ability of the microphone array to suppress the physically high sound pressure levels at the points close to the microphones, therefore, an optimised weighting strategy is introduced and applied.

Acknowledgements

The authors gratefully acknowledge the European Commission for its support of the Marie Sklodowska Curie program through the ETN PBNv2 project (GA 721615).

References

[1] *Measurement of noise emitted by accelerating road vehicles -- Engineering method -- Part 1: M and N categories* (ISO362-1:2015).

[2] *Measurement of noise emitted by accelerating road vehicles -- Engineering method -- Part 1: M and N categories* (ISO362-1:2016)

[3] A. Schuhmacher, Y. Shirahashi, M. Hirayama, Y. Ryu, *Indoor pass-by noise contribution analysis using source path contribution concept*, Proceedings of the 2012 International Conference on Modal Analysis Noise and Vibration Engineering (ISMA 2012), Leuven, pp. 3697-3709.

[4] U. Kim, M. Maunder, D. Mawdsley, P. Grant, *Simulation Method to meet new pass-by noise requirements*, Sound & Vibration/September 2015

[5] M. Kramer, P. Brandstatt, A. Ickinger, *Comparison of pass-by noise from real track and simulated measurement at the roller test bench*, Inter Noise 2016, Hamburg

[6] S. Guidati, R. Sottek, K. Genuit, *Simulated pass-by in small rooms using noise synthesis technology*, CFA/DAGA 2004, Strasbourg

[7] F. Fahy, D. Thompson, *Fundamentals of Sound and Vibration: Second Edition*, CRC Press, 2015